RSC Advances

PAPER

View Article Online
View Journal | View Issue

Cite this: *RSC Adv.*, 2021, **11**, 33522

Preparation, characterization of spherical 1,1-diamino-2,2-dinitroethene (FOX-7), and study of its thermal decomposition characteristics

Xinhua Zhao,[a] Dan He,[b] Xiaoping Ma,[b] Xueying Liu,[b] Zishuai Xu,[b] Lizhen Chen *[a] and Jianlong Wang[a]

The sensitivity and properties of energetic materials strongly depend on their crystal morphology. In this article, spherical 1,1-diamino-2,2-dinitroethylene (FOX-7) was produced *via* a combination of the cooling crystallization method and repeated grinding technique. X-ray diffraction (XRD), Fourier-transform infrared spectroscopy (FT-IR), optical microscopy, scanning electron microscopy (SEM) and laser particle size analysis were used to characterize the structure, infrared characteristics, morphology, and particle size of the product. The results show that the obtained product has a smoother spherical morphology with granularity gradation and shows similar diffraction peak positions to raw FOX-7. Differential scanning calorimetry (DSC), thermal gravimetry (TG), and accelerating rate calorimetry (ARC) were used to analyse the thermal behavior of spherical FOX-7 under nonisothermal and adiabatic conditions. The thermal performance test results show that spherical FOX-7 releases energy faster and releases more energy as compared to raw FOX-7. These findings showed that the cooling crystallization method combined with the repeated grinding technique is suitable for efficient preparation of spherical FOX-7, which could greatly improve the thermal stability of FOX-7.

Received 1st August 2021
Accepted 5th October 2021

DOI: 10.1039/d1ra05836c

rsc.li/rsc-advances

1. Introduction

In recent years, countries all over the world have been actively developing solid propellants based on new energetic materials that have theoretically high efficacy and potentially meet the requirements of low vulnerability, which has promoted the research and development of high-energy insensitive explosives. The shortcomings of irregular crystal morphology, rough surface, relatively large aspect ratio, and agglomeration will seriously affect the performance of explosives in propellants.[1] The crystal morphology of explosives not only has a direct impact on its process performance, but also has an important impact on its chemical properties and explosive performance. Studies have shown that the crystal morphology is regular and close to spherical,[2] which can increase the density and dispersion of explosives, thereby improving the mechanical properties and mechanical sensitivity of the medicine column.

1,1-Diamino-2,2-dinitroethene (better known as FOX-7), is a thermally stable insensitive munition (IM) high-energy material first reported by the FOA Defence Research Establishment (Sweden) in 1998.[3] As shown in Fig. 1, FOX-7 has symmetrical molecular components and infinite two-dimensional wavy single-layer molecular fillers, and its special structure determines some of the physicochemical properties, in particular its low solubility, low sensitivity to friction and impact, and the absence of the melting point.[4,5] The detonation speed of FOX-7 is equivalent to RDX and HMX; the sensitivity is lower than RDX and HMX, and is equivalent to TATB.[6] All kinds of excellent properties make FOX-7 expected to become one of the main candidate varieties and components of insensitive explosives in the future.

In order to produce spherical FOX-7, various research activities have been carried out at home and abroad. Alok Kumar Mandal *et al.*[2] prepared sub-micron spherical FOX-7 using a micellar nanoreactor, and the impact sensitivity was slightly improved. Ruixuan Xu *et al.*[7] prepared nano-spherical FOX-7 by mechanical ball milling. The sensitivity of nano-spherical FOX-7 particles is reduced, and the thermal stability is improved as compared to raw FOX-7. Yuanping Zhang *et al.*[8] used spray-drying method to prepare nanoparticle-stacked FOX-7 microspheres. The particle size of the microspheres FOX-7 formed by stacking nanoparticles (100–250 nm) is 1–5 μm, which is significantly smaller than the raw FOX-7. Particle size reduction of energetic materials has some advantages and some disadvantages.[9] It was found that whilst nanosizing of explosives leads to a reduction in their sensitivity to external stimuli, it often leads to reduced shelf life. Therefore, the storage and handling of propellants containing nano energetic materials will be accompanied by hazards.[10] However, in contrast, the cooling crystallization method by soaking the sample in a mixed

[a]*School of Chemical Engineering and Technology, North University of China, Taiyuan 030051, China. E-mail: Chen17555@163.com*

[b]*Research Institute of Gan Su Yin Guang Chemical Industry Group, Baiyin 730900, China*

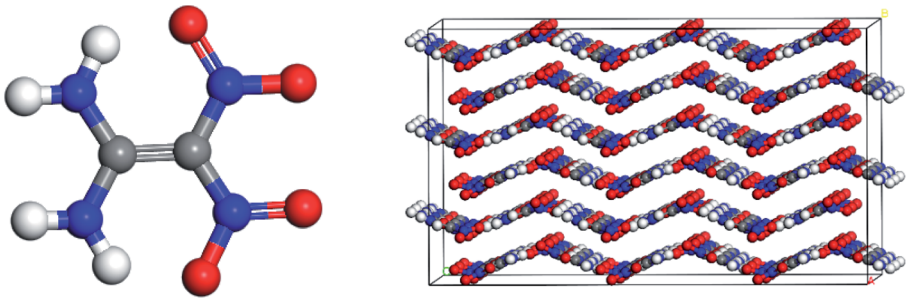

Fig. 1 Molecular structure and molecular stacking of FOX-7 (gray: C; white: H; red: O; blue: N).

solvent with stirring is simpler and more economical for large-scale preparation.[11] The explosive crystal obtained by the recrystallization method has the characteristics of high purity and high quality. Repeated grinding technique is a completely physical process that can achieve low-cost and mass production, and it will not cause environmental pollution.

After the necessary characterization of the explosive obtained by the crystallization, it is necessary to study its kinetics of thermal decomposition reaction to provide supporting data for future applications in weapon systems.[12] Differential scanning calorimetry (DSC), thermal gravimetric (TG), and accelerating rate calorimeter (ARC) are commonly used methods to study the thermal decomposition behavior of energetic materials. In this study, spherical FOX-7 was successfully fabricated from the raw FOX-7 *via* a combination of cooling crystallization method and repeated grinding technique. The spherical FOX-7 crystal morphology, size, structure, and thermal behavior were systematically investigated in detail. It was quite useful to the evaluation of chemical properties of prepared spherical FOX-7 and to the study of its thermal changes at high temperatures.

2. Experiment

2.1 Materials

Raw FOX-7 has a purity of greater than 99.5% by HPLC and was provided by Xi'an Modern Chemistry Research Institute.[13] Dimethyl sulfoxide (C_2H_6OS, AR grade, abbreviated as DMSO) and acetone (C_3H_6O, AR grade, abbreviated as ACE) were purchased from Shanghai Titan Scientific Co., Ltd. and Tianjin Shentai Chemical Reagent Co., Ltd., respectively. All reagents were used without further purification.

2.2 Preparation of spherical of FOX-7

The core content is the two-step preparation technology of raw FOX-7 through cooling crystallization and repeated grinding, using the principle of preferential dissolution of particle edges and the friction caused by the collision of particles in the solvent to obtain spherical FOX-7 crystals.

FOX-7 is hardly soluble in water and common organic solvents, but easily soluble in strong polar solvents such as DMSO.[14] We used a mixture of DMSO and ACE to recrystallized FOX-7. It specifically includes the following steps: (1) add FOX-7 and mixed solvent (V_{DMSO}/V_{ACE} = 2/1) into the crystallization kettle to dissolve it fully, and the initial temperature of the crystallization kettle is 60 °C; (2) lower the temperature of the crystallization kettle while stirring to form a supersaturated solution and then crystal nucleus generate and grow, culture crystal 3 hours; (3) cool down to room temperature while stirring; (4) stir for 3 days at room temperature, so that the produced crystals are repeatedly ground in the crystallization mother liquor; (5) filter, wash with ACE, and dry to obtain spherical FOX-7 crystals. The crystallization process conditions involved in the preparation method are simple and easy to control. The crystallization mother liquor can be recycled, which is beneficial to reduce the environmental pollution of organic solvents. Low cost, safe and reliable, suitable for industrialized mass production.

2.3 Characterization

X-ray diffraction (XRD) of FOX-7 was collected on a Bruker D8-Advanced eco diffractometer in the 2θ range of 5–60° with Cu Kα radiation (λ = 1.5418 Å) operated at 40 kV and 25 mA. Fourier-transform infrared spectroscopy (FT-IR) of FOX-7 was collected on a VERTEX 80 produced by Bruker (Germany).

The morphology of FOX-7 was characterized by optical microscopy (Shanghai Optical Instrument Factory, XSP-10A type, China) and scanning electron microscope (Phenom,

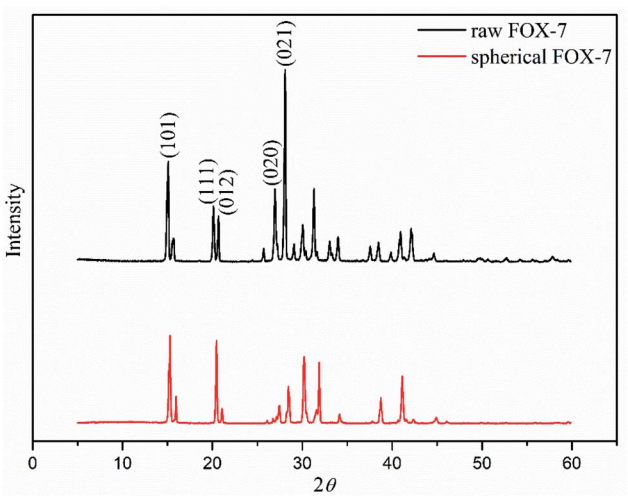

Fig. 2 XRD patterns of raw FOX-7 and spherical FOX-7.

Pure, Netherlands). The particle size distribution of FOX-7 was characterized by laser particle size analyzer (Dandong Baite Instrument Co., Ltd., BT-2002 type, China).

2.4 Thermal behavior

2.4.1 Nonisothermal tests by TG and DSC. The coupled TG-DSC technique (TGA/DSC 3+, Mettler Toledo, Switzerland) has been applied for analyzing the thermal decomposition process of spherical FOX-7. For a comparison, raw FOX-7 was also put into the measurement. The conditions of TG-DSC were as follows: each sample was 0.9 mg and placed in an open alumina crucible from 100 to 400 °C at the heating rate of 10 K min^{-1} under N_2 flow rate of 50 mL min^{-1}.

DSC is a common equipment used to measure various thermodynamic and kinetic parameters of energetic materials.[15] The DSC measurements were carried out with a METTLER DSC 3 instrument (Switzerland). The conditions of DSC were as follows: each sample was 0.9 mg and placed in an aluminum crucible with a pinhole cover from 100 to 300 °C at the heating rate of 5, 10, 15 and 20 K min^{-1} under N_2 flow rate of 50 mL min^{-1}.

2.4.2 Adiabatic tests by ARC. ARC is a thermal analysis instrument designed based on the adiabatic principle.[16,17] The ARC measurements were carried out with an ES-ARC instrument (England). The sample ball used for the test is a titanium alloy ball, the mass is 8.5696 g, and the specific heat capacity is 0.523 J g^{-1} $°C^{-1}$. The conditions of ARC were as follows: procedure: heat-wait-search (H–W–S); temperature range: 120–400 °C; heating step: 5 °C; waiting time: 15 minutes; temperature rate sensitivity: 0.02 K min^{-1}; sample mass: 0.0835 g.

3. Results and discussion

3.1 XRD and FT-IR

XRD and FT-IR were adopted to identify the crystalline phase of raw FOX-7 and spherical FOX-7. And the results are as follows.

Fig. 2 shows the XRD patterns of raw FOX-7 and spherical FOX-7. Raw FOX-7 displays five typical peaks which are assigned to the (1 0 1), (1 1 1), (0 1 2), (0 2 0), (0 2 1) growth planes, and crystal form of FOX-7 is α-phase.[18] It is noticed that the typical peaks of spherical FOX-7 are consistent with the peaks of raw FOX-7, indicating that the crystal structure of spherical FOX-7 does not change during the two processes of cooling crystallization and repeated grinding.

In Fig. 3, FT-IR spectra of raw FOX-7 and spherical FOX-7 showed absorbance in the ~3220–3416 cm^{-1} and ~1332–1620 cm^{-1} wavenumber ranges characteristic of the $–NH_2$ and $–NO_2$ functional groups and numerous peaks in the fingerprint region.[19] FT-IR spectra of spherical FOX-7 were consistent with those of raw materials, indicating that FOX-7 did not change during the two processes of cooling crystallization and repeated grinding.

3.2 Morphology and size

Explosive particle grading refers to the proportion of solids with different particle sizes that match each other. Relevant literature reports indicate that particle size grading can improve the

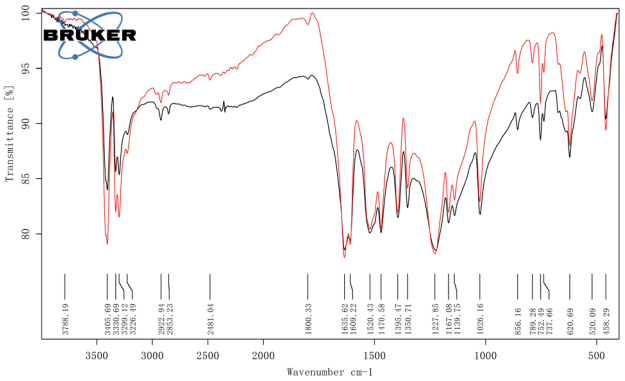

Fig. 3 FT-IR spectra of raw FOX-7 (black line) and spherical FOX-7 (red line).

formability of explosives,[20,21] increase the density and compressive strength of explosives, and improve the mechanical properties of explosives. Within a certain range, the output energy, detonation pressure, and compressive strength of the explosives increase with the increase of the charge density, and the particle size grading is a very effective way to improve the packing density. Therefore, it is of great significance to develop low-sensitivity high-energy explosives and study the particle size grading technology of explosives.[22]

The optical microscope images, scanning electron microscope images, and particle size distribution curves were shown in Fig. 4–6, respectively. Raw FOX-7 appeared as irregular fines with conspicuous edges and corners. The average particle size (d_{50}) of raw FOX-7 is 59.26 μm with a narrow particle size distribution (d_3 represents the diameter corresponding to 3% of the cumulative particle size distribution, and its value is 21.80 μm; d_{98} represents the diameter corresponding to 98% of the cumulative particle size distribution, and its value is 148.55 μm). After the cooling crystallization and repeated grinding process, the spherical FOX-7 with a uniform texture, few crystal deficiencies, and good dispersion, was obtained. The average particle size (d_{50}) of spherical FOX-7 is 322.91 μm with a rather broad size distribution ($d_3 = 20.18$ μm, $d_{98} = 981.65$ μm). The spherical FOX-7 particle size distribution curve has three peaks, showing a particle size gradation. The gaps between particles of different particle sizes are filled with each other, which can increase the density of the explosive, thereby increasing the detonation speed.

The concept of sphericity is introduced to quantitatively describe the sphericity of particle shape, as shown in eqn (1).[23]

$$\varphi_s = \frac{L}{S} \quad (1)$$

where φ_s is the sphericity of the particle, L is the radius of long axis of the particle, and S is the radius of short axis of the particle. The sphericity of the spherical FOX-7 prepared by measurement is in the range of 1.00 to 1.36.

3.3 Thermal decomposition characteristics

3.3.1 Thermal analysis by TG and DSC. Thermal analysis of spherical FOX-7 and raw FOX-7 were carried out in TG-DSC. The

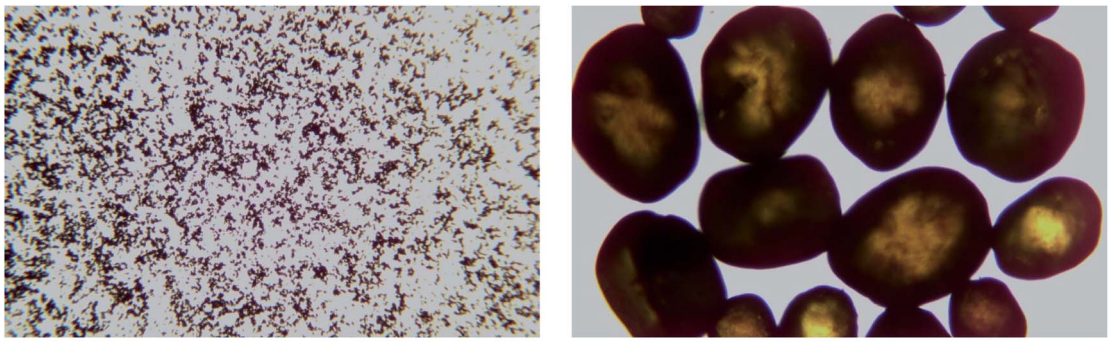

a. raw FOX-7 b. spherical FOX-7

Fig. 4 Optical microscopy images (×40) of raw FOX-7 and spherical FOX-7.

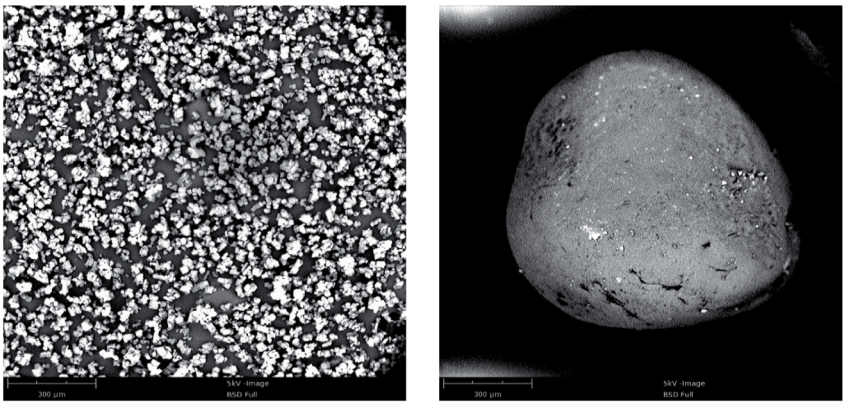

a. raw FOX-7 b. spherical FOX-7

Fig. 5 Scanning electron microscope images of raw FOX-7 and spherical FOX-7.

TG-DSC curves of raw FOX-7 and spherical FOX-7 decomposed at the heating rate of 10 K min^{-1} are shown in Fig. 7 and 8, respectively.

As we can see in Fig. 7, the TG curve displays two-stage mass loss in which the first stage began around 219.49 °C and completed at 242.20 °C accompanied with 33.3% mass loss. The second stage completed at 306.50 °C accompanied with 54.8% mass loss. DSC curve of raw FOX-7 exhibits one endothermic peak and two exothermic peaks, identical to the TG results. The temperature of the endothermic peak at 116.51 °C corresponds to the phase transition from α to β. The first decomposition peak temperature was 231.27 °C is mainly due to the breakage of the intra- and intermolecular hydrogen bonds of FOX-7 under heating. The adjacent FOX-7 molecules remove two amino hydrogen and one nitro oxygen to formation of water molecules, with the condensation reaction of carbon–carbon double bonds.[24] The second decomposition peak temperature was 297.95 °C, which is mainly owing to the fracture of the carbon skeleton in FOX-7.[19,25]

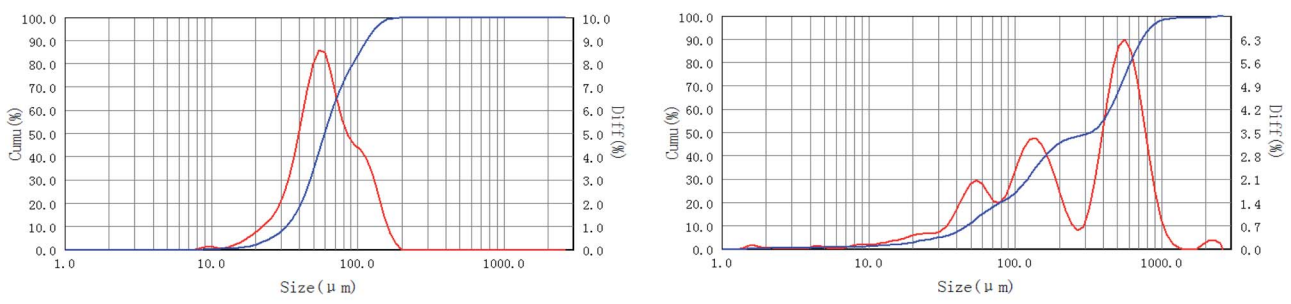

a. raw FOX-7 b. spherical FOX-7

Fig. 6 Particle size distribution curves of raw FOX-7 and spherical FOX-7 (red line: particle size; blue line: content).

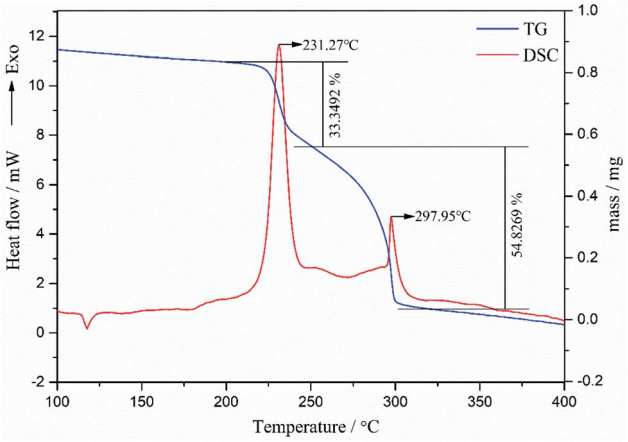

Fig. 7 TG-DSC curves of raw FOX-7.

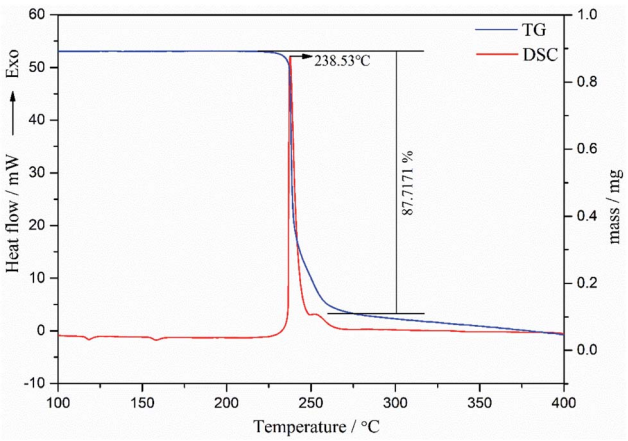

Fig. 8 TG-DSC curves of spherical FOX-7.

As can be seen from Fig. 8, the TG curve displays one-stage mass loss in which the stage began around 229.52 °C and completed at 248.78 °C accompanied with 87.7% mass loss. DSC curve of spherical FOX-7 exhibits two endothermic peaks and one exothermic peak, identical to the TG results. The first endothermic peak (117.29 °C) for the $\alpha \rightarrow \beta$ phase transition and the second endothermic peak (157.61 °C) for the $\beta \rightarrow \gamma$ transition,[9,26] which confirmed that the DSC crystal form transition peak of FOX-7 is related to the particle size of the sample.[27] It should be noted that, compared with raw FOX-7, the two steps of spherical FOX-7 almost merging into a single peak (238.53 °C).[28] Ostmark *et al.*[29] explained the differences between the individual DSC curves of FOX-7 by proposing the relationship between particle size and decomposition temperature.

The DSC curves of spherical FOX-7 carried out at different heating rates are shown in Fig. 9. For different heating rates 5, 10, 15, and 20 K min^{-1} of spherical FOX-7, four different values of the peak temperature of 242.22, 246.11, 249.54, and 251.77 °C were obtained, respectively. As can be seen, both the decomposition onset temperature and exothermic peak temperature increase with the increase of the heating rate. This is because

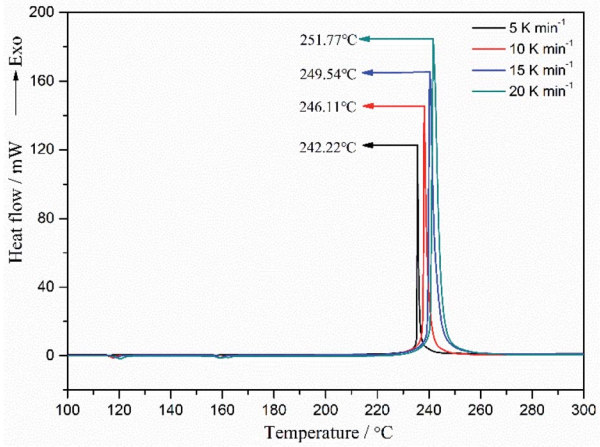

Fig. 9 DSC curves of spherical FOX-7.

the temperature rises too fast, the reaction has not been carried out, and the higher temperature is entered, causing the reaction to lag.

To achieve the effective evaluation and better functionality of spherical FOX-7, it was necessary to estimate the thermal decomposition kinetic parameters.[30] The apparent activation energy (E) and pre-exponential constant (A) of spherical FOX-7 were calculated by Kissinger method (eqn (2)) and Ozawa method (eqn (3)).[31,32] The critical initiation temperature (T_b) is defined as the lowest temperature at which a specific charge can be heated without thermal runaway.[33–36] The initial decomposition temperature (T_{P_0}) in the exothermic decomposition process corresponding to $\beta \rightarrow 0$.[37,38] The activation entropy ($\Delta S^{\neq}$), activation enthalpy ($\Delta H^{\neq}$), and activation Gibbs free energy ($\Delta G^{\neq}$) can reflect the difference between the activated transition state and the initial reactant in the rate-determining reaction of thermal decomposition. The $\Delta S^{\neq}$, $\Delta H^{\neq}$, $\Delta G^{\neq}$, and T_b at T_{P_0} can be calculated based on eqn (4)–(8).[39,40]

$$\ln\left(\frac{\beta_i}{T_{P_i}^2}\right) = \ln\left(\frac{AR}{E}\right) - \frac{E}{RT_{P_i}} (i = 1-4) \quad (2)$$

$$\lg \beta_i = \lg\left[\frac{AE}{RG(\alpha)}\right] - 2.315 - \frac{0.4567E}{RT_{P_i}} (i = 1-4) \quad (3)$$

$$T_{P_i} = T_{P_0} + b\beta_i + c\beta_i^2 + d\beta_i^3 \ (i = 1\text{–}4) \quad (4)$$

$$A_k = \frac{k_B T}{h} \exp\left(\frac{\Delta S^{\neq}}{R}\right) \quad (5)$$

$$\Delta H^{\neq} = E_k - RT_{P_0} \quad (6)$$

$$\Delta G^{\neq} = \Delta H^{\neq} - T\Delta S^{\neq} \quad (7)$$

$$T_b = \frac{E_k - \sqrt{E_k^2 - 4E_k RT_{P_0}}}{2R} \quad (8)$$

where β is the heating rate, K min^{-1}; T_P is the peak temperature, K; A is the pre-exponential constant, s^{-1}; R is the gas constant, 8.314 J mol^{-1} K^{-1}; E is the apparent activation energy, J mol^{-1};

Table 1 Decomposition kinetics basic data of spherical FOX-7 by DSC

			Kissinger method	Ozawa method
β/K min^{-1}	T_P/K	$10^3\ T_P^{-1}$/K^{-1}	$\ln(\beta/T_P^2)$/min^{-1} K^{-1}	lg β/K min^{-1}
5	515.37	1.9404	−10.8803	0.6990
10	519.26	1.9258	−10.2022	1.0000
15	522.69	1.9132	−9.8099	1.1761
20	524.92	1.9051	−9.5308	1.3010

Table 2 Kinetics parameters of spherical FOX-7

Kissinger method			Ozawa method				Thermodynamic parameters at T_0		
E_k/kJ mol^{-1}	A/s^{-1}	r_k^2	E_o/kJ mol^{-1}	r_o^2	T_{P_0}/K	T_b/K	$\Delta S^{\neq}$/J mol^{-1} K^{-1}	$\Delta H^{\neq}$/kJ mol^{-1}	$\Delta G^{\neq}$/kJ mol^{-1}
314.03	5.03×10^{31}	0.9904	306.82	0.9909	511.76	518.89	357.50	309.77	126.82

Table 3 Comparison of kinetics parameters of raw FOX-7 (ref. 41) and spherical FOX-7

	Kissinger method				Thermodynamic parameters at T_0		
Sample	E/kJ mol^{-1}	A/s^{-1}	T_{P_0}/K	T_b/K	$\Delta S^{\neq}$/J mol^{-1} K^{-1}	$\Delta H^{\neq}$/kJ mol^{-1}	$\Delta G^{\neq}$/kJ mol^{-1}
Raw FOX-7	249.89	4.50×10^{30}	485.05	486.70	337.85	249.89	85.90
Spherical FOX-7	314.03	5.03×10^{31}	511.76	518.89	357.50	309.77	126.82

$G(\alpha)$ is an integral form of reaction mechanism function; k_B is the Boltzmann constant, 1.3807×10^{-23} J K^{-1}; h is the Planck constant, 6.626×10^{-34} J s.

Decomposition kinetics basic data of spherical FOX-7 is listed in Table 1. The calculated thermal decomposition kinetics parameters are shown in Table 2. It can be found that the linear correlation coefficients of the two methods are both greater than 0.99, indicating that the measurement data is accurate and reliable. The apparent activation energy (E) is 314.03 kJ mol^{-1} and pre-exponential constant (A) is 5.03×10^{31} s^{-1}, obtained by the Kissinger method. The apparent activation energy (E) is 306.82 kJ mol^{-1} obtained by the Ozawa method. The values of E obtained by the two methods are very close, proving that the two methods were appropriate for activation energy threshold calculations. Compared with the raw FOX-7 (Table 3),[41] both apparent activation energy (E) and critical initiation temperature (T_b) of spherical FOX-7 are all increased, and the pre-exponential constant (A) also have a corresponding increase. This indicates that under thermal stimulation, spherical FOX-7 is more difficult to decompose than raw FOX-7, and the spherical outer shape effectively improves the thermal stability of FOX-7. The increased activation entropy ($\Delta S^{\neq}$) value indicated a higher degree of disorder of spherical FOX-7 compared to that of raw FOX-7. The larger value of activation enthalpy ($\Delta H^{\neq}$) for spherical FOX-7 results in their faster reaction rates. The positive value of activation Gibbs free energy ($\Delta G^{\neq}$) indicates a nonspontaneous process. These data can be used as basic data for studying the physical and chemical properties of spherical FOX-7 and for theoretical calculations.[42]

3.3.2 Thermal analysis by ARC. The thermal stability analysis of spherical FOX-7 under adiabatic conditions was carried out by using ARC. Temperature and pressure *versus* time and dT/dt and dP/dt *versus* time curves of spherical FOX-7 are shown in Fig. 10 and 11, respectively. The measured data of the spherical FOX-7 decomposition stage are shown in Table 4.

Since the heat released by the decomposition reaction of the sample is used not only for heating itself, but also for heating

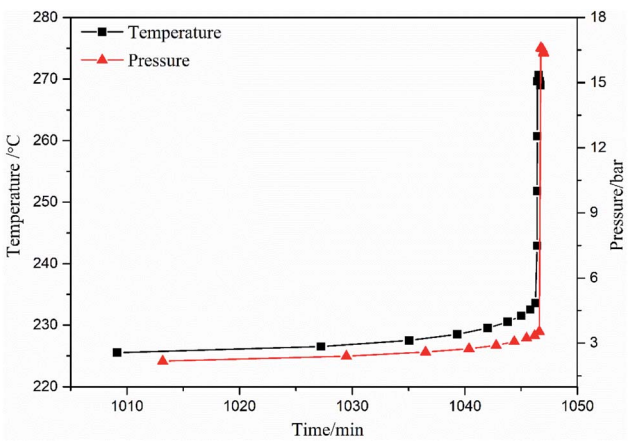

Fig. 10 Temperature and pressure *versus* time curves of spherical FOX-7.

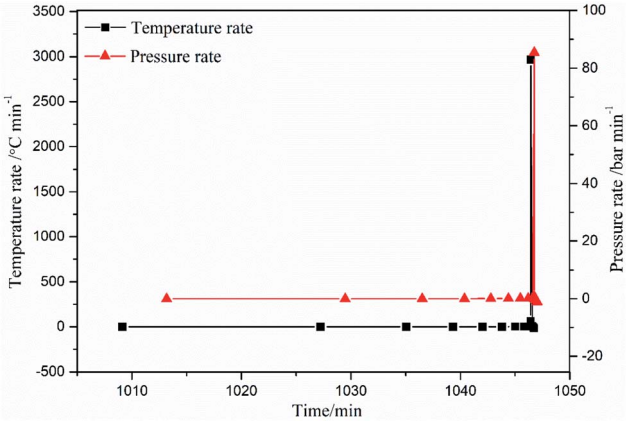

Fig. 11 dT/dt and dP/dt *versus* time curves of spherical FOX-7.

Table 4 Measured and corrected thermal decomposition parameters of spherical FOX-7 by ARC

Parameters	Values	Corr.
Onset temperature/°C	225.50	—
Onset temperature rate/K min^{-1}	0.02	0.94
Max self-heating rate/K min^{-1}	2970.96	138 907.91
Temperature at max rate/°C	269.64	—
Final temperature/°C	270.67	2337.43
Adiabatic temperature rise/°C	45.17	2111.93
Time to maximum rate/min	1046.43	22.38
Onset pressure/bar	2.17	—
Pressure at max rate/bar	16.60	—

the sample ball, the test result is the entire reaction system composed of the sample and the sample ball. When all the heat released by the sample reaction is used to heat itself, the actual temperature rise and temperature rate of the sample are higher than the test value.[43] Therefore, the thermal decomposition parameters measured in Table 4 need to be corrected. The corresponding equations are listed as follows:[44]

$$\Phi = 1 + \frac{M_b \times C_{Vb}}{M \times C_V} \quad (9)$$

$$\Delta T_S = \Phi \Delta T \quad (10)$$

$$m_{0s} = \Phi m_0 \quad (11)$$

$$T_{fs} = T_0 + \Phi \Delta T \quad (12)$$

$$\theta_S = \frac{\theta}{\Phi} \quad (13)$$

where M_b and M are the mass of bomb and sample, respectively; C_{vb} and C_v are the specific heat of bomb and sample, respectively; ΔT is the adiabatic temperature rise; m_0 is the initial self-heating rate; T_0 is the initial decomposition temperature; θ is the time-to-maximum rate; subscript s is the corrected value.

It can be seen from Fig. 10, 11 and Table 4 that the values of temperature (temperature rate) and pressure (pressure rate) were small at the beginning, but increased suddenly when the temperature exceeded 233 °C. The temperature rose from 233.57 °C to 269.64 °C within 0.162 min, the corresponding temperature rates were 2.28 K min^{-1} and 2970.96 K min^{-1}, and the pressure rose from 3.53 bar to 16.60 bar. The reaction system reached the maximum temperature rate of 2970.96 K min^{-1} at 269.64 °C. After 0.132 minutes, the system reached the maximum temperature of 270.67 °C, and then the temperature rate became negative, and the system temperature began to drop. During the thermal decomposition of spherical FOX-7, the maximum pressure measured by the system was 16.60 bar. The high pressure and self-heating rate indicated that the energy released by the runaway reaction of spherical FOX-7 is very large. If it decomposes uncontrollably in a confined space, it may cause fire, deflagration, or even explosion.[45]

4. Conclusions

In conclusion, we have developed a facile approach to prepare spherical FOX-7 *via* a combination of cooling crystallization method and repeated grinding technique. The novel, simple and effective method was confirmed that can provide regular spherical FOX-7 with smoother surface and uniform dispersion. The average particle size of spherical FOX-7 is 322.91 μm, and its particle size distribution curve has three peaks showing a particle size gradation, which may be helpful for the potential use in military and industrial applications. The thermal decomposition of spherical FOX-7 by TG, DSC, and ARC was reported in detail. The results show that spherical FOX-7 shows more remarkable thermal stability, release energy faster and release more energy as compared to raw FOX-7. This article provides key thermodynamic, and chemical kinetic parameters for the mathematical model of the combustion process, and provides a theoretical basis for the energy prediction and safe storage performance of prepared spherical FOX-7.

Author contributions

Xinhua Zhao: conceptualization, investigation, data curation, validation, writing – original draft. Dan He: conceptualization, resources. Xiaoping Ma: software, validation. Xueying Liu: supervision, funding acquisition. Zishuai Xu: methodology, supervision. Lizhen Chen: conceptualization, methodology, writing – review & editing. Jianlong Wang: resources, project administration, funding acquisition.

Conflicts of interest

There are no conflicts to declare.

References

1 X. T. Ren, D. Y. Ye, N. Ding, J. X. He, Y. H. Lu, Q. Lei, *et al.*, A Molecular Dynamics Simulation of Solvent Effects on the Crystal Morphology of FOX-7, *Acta Armamentarii*, 2015, **36**(2), 272–278.

2 A. K. Mandal, U. Thanigaivelan, R. K. Pandey, S. Asthana, R. B. Khomane and B. D. Kulkarni, Preparation of Spherical Particles of 1,1-Diamino-2,2-dinitroethene (FOX-7) Using a Micellar Nanoreactor, *Org. Process Res. Dev.*, 2012, **16**(11), 1711–1716.

3 N. V. Latypov, J. Bergman, A. Langlet, U. Wellmar and U. Bemm, Synthesis and reactions of 1,1-diamino-2,2-dinitroethylene, *Tetrahedron*, 1998, **54**(38), 11525–11536.

4 U. Bemm and H. Östmark, 1,1-Diamino-2,2-dinitroethylene: A Novel Energetic Material with Infinite Layers in Two Dimensions, *Acta Crystallogr.*, 2014, **154**(12), 997–1999.

5 H. Ostmark, A. Langlet and H. Bergman, *FOX-7 - A new explosive with low sensitivity and high performance, 11th International Symposium on Detonation*, Snowmass, USA, 1998.

6 Z. K. Long, Research development of 1,1-Diamino-2,2-dinitroethylene synthesis, *Guangzhou Chem.*, 2013, **38**(4), 71–78.

7 R. X. Xu, C. W. An, H. Huang, J. Y. Wang, B. Y. Ye and B. Liu, Preparation of multi-scale FOX-7 particles and investigation of sensitivity and thermal stability, *RSC Adv.*, 2019, **9**(36), 21042–21049.

8 Y. P. Zhang, C. H. Hou, X. L. Jia, J. Wang and Y. Tan, Fabrication of Nanoparticle-Stacked 1,1-Diamino-2,2-Dinitroethylene (FOX-7) Microspheres with Increased Thermal Stability, *J. Nanomater.*, 2019, **1**, 1–9.

9 B. Huang, M. H. Cao, F. D. Nie, H. Huang and C. W. Hu, Construction and Properties of Structure- and Size-controlled Micro/nano-Energetic Materials, *Def. Technol.*, 2013, **9**, 59–79.

10 N. Zohari, M. H. Keshavarz and S. A. Seyedsadjadi, The Advantages and Shortcomings of Using Nano-sized Energetic Materials, *Cent. Eur. J. Energ. Mater.*, 2013, **10**(1), 135–147.

11 P. Pandita, V. P. Arya and G. Kaur, Particle size reduction of RDX by sequential application of solvent-antisolvent recrystallization and mechanical methods, *J. Energ. Mater.*, 2020, **38**, 309–325.

12 Z. H. Liu, *Introduction to Thermal Analysis*, Chemical Industry Press, Beijing, 1st edn, 1991.

13 L. Hu, M. Zhang, C. Zhou and H. Y. Tian, Determination of the Purity of FOX-7 by Reversed Phase HPLC, *Chin. J. Explos. Propellants*, 2005, **3**, 87–88.

14 X. H. Zhao, D. L. Cao, J. L. Wang, L. Z. Chen, Y. Y. Zhang and C. Zhou, Solubility and Crystallization of FOX-7 in DMSO-H_2O, DMSO-EtOH and DMSO-ACE Binary Mixed Solvents, *Chin. J. Explos. Propellants*, 2019, **4**(5), 473–479.

15 N. Unidas, *Recommendations on the transport of dangerous goods, Committee of experts on the transport of dangerous goods*, UN, 1995.

16 S. V. Pakkirisamy, S. Mahadevan, S. S. Paramashivan and A. B. Mandal, Adiabatic thermokinetics and process safety of pyrotechnic mixtures: atom bomb, Chinese, and palm leaf crackers, *J. Therm. Anal. Calorim.*, 2012, **109**, 1387–1395.

17 J. C. Tou and L. F. Whiting, The thermokinetic performance of an accelerating rate calorimeter, *Thermochim. Acta*, 1981, **48**(1–2), 21–42.

18 H. Cai, L. Tian, B. Huang, G. Yang, D. Guan and H. Huang, 1,1-Diamino-2,2-dintroethene (FOX-7) nanocrystals embedded in mesoporous carbon FDU-15, *Microporous Mesoporous Mater.*, 2013, **170**, 20–25.

19 B. Gao, P. Wu and B. Huang, Preparation and characterization of nano-1,1-diamino-2,2-dinitroethene (FOX-7) explosive, *New J. Chem.*, 2014, **38**(6), 2334–2341.

20 C. L. Lv, Experimental and theoretical research on the particle size and particle size grading of the main explosive and the shock wave sensitivity and energy output of the explosive, Master's thesis, North China Institute of Technology, Taiyuan, 2001.

21 S. R. Yun, *Preliminary study on the gradation law of hexogen particles*, National Defense Industry Press, 1964.

22 Q. A. Huang, Q. Z. Cui, C. W. Zhao and L. Ning, Optimization Particle Grading of Explosive Based on Dense Packing, *Sci. Technol. Eng.*, 2015, **15**(25), 130–134.

23 T. Fan, Numerical simulation study on the sphericity separation process of coated nuclear fuel particles, Master's thesis, Zhejiang Univ., Hangzhou, 2021.

24 A. Gindulyte, L. Massa, L. Huang and J. Karle, Proposed Mechanism of 1,1-Diamino-Dinitroethylene Decomposition: A Density Functional Theory Study, *J. Phys. Chem. A*, 1999, **103**(50), 11045–11051.

25 D. E. Taylor, F. Rob, B. M. Rice, R. Podeszwa and K. Szalewicz, A molecular dynamics study of 1,1-diamino-2,2-dinitroethylene (FOX-7) crystal using a symmetry adapted perturbation theory-based intermolecular force field, *Phys. Chem. Chem. Phys.*, 2011, **13**(37), 16629–16636.

26 K. Chatragadda and A. A. Vargeese, A Kinetics Investigation on the Nitro-Nitrite Rearrangement Mediated Thermal Decomposition of High Temperature Monoclinic Phase of 1,1-Diamino-2,2-Dinitroethylene (γ-FOX-7), *J. Chem. Sci.*, 2017, **129**, 281–288.

27 Q. B. Fu, Y. J. Shu, Y. G. Huang, J. H. Zhou and Y. X. Zhang, Preparation and thermal properties of FOX-7 crystal, *Journal of Propellants and Explosives*, 2009, **32**(4), 6–9.

28 I. J. Lochert, *FOX-7 - A new insensitive explosive*, DSTO Aeronautical and Maritime Research Laboratory, Australia, 2001.

29 H. Ostmark, H. Bergman and U. Bemm, in *2,2-dinitro-ethene-1,1-diamine (FOX-7) - properties, analysis and scale-up, 32nd International Annual Conference of ICT on Energetic Materials - Ignition, Combustion and Detonation*, Karlsruhe, Germany, 2001.

30 M. Zhang, F. Q. Zhao, Y. J. Yang, J. K. Zhang, N. Li and H. X. Gao, Effect of rGO–Fe_2O_3 nanocomposites fabricated in different solvents on the thermal decomposition properties of ammonium perchlorate, *CrystEngComm*, 2018, **20**, 7010–7019.

31 H. E. Kissinger, Reaction Kinetics in Differential Thermal Analysis, *Anal. Chem.*, 1957, **29**(11), 1702–1706.

32 T. A. Ozawa, A New Method of Analyzing Thermo-gravimatric Data, *Bull. Chem. Soc. Jpn.*, 1965, **38**, 1881–1886.

33 T. L. Zhang, R. Z. Hu, Y. Xie and F. Li, The estimation of critical temperatures of thermal explosion for energetic

materials using non-isothermal DSC, *Thermochim. Acta*, 1994, **244**, 171–176.

34 A. K. Burnham, R. K. Weese, A. P. Wemhoff and J. L. Maienschein, A historical and current perspective on predicting thermal cook-off behavior, *J. Therm. Anal. Calorim.*, 2007, **89**(2), 407–415.

35 J. M. Pickard, Critical Ignition Temperature, *Thermochim. Acta*, 2002, **392**(2), 37–40.

36 Q. Ma, H. C. Lu, L. Y. Liao, G. Fan and J. Huang, One-Pot Synthesis, Crystal Structure, and Thermal Decomposition Behavior of 1,1′-Diamino-4,4′,5,5′-Tetranitro-2,2′-Biimidazole, *J. Energ. Mater.*, 2016, **35**(2), 1–11.

37 Y. Yue, X. D. Li, Y. T. Sun, J. A. Tian, H. M. Liu, B. D. Wu, *et al.*, Preparation and characterization of HMX/EVA/hBNNSs micro-composites with improved thermal stability and reduced sensitivity, *Def. Technol.*, 2021, **17**, 650–656.

38 R. Z. Hu, S. L. Gao and F. Q. Zhao, *Thermal analysis kinetics*, Science Press, Beijing, 2nd edn, 2008.

39 M. T. Hosamani, N. H. Ayachit and D. K. Deshpande, Activation energy ($\Delta G^{\neq}$), enthalpy ($\Delta H^{\neq}$), and entropy ($\Delta S^{\neq}$) of some indoles and certain of their binary mixtures, *J. Therm. Anal. Calorim.*, 2012, **107**, 1301–1306.

40 P. L. Houston, *Chemical Kinetics and Reaction Dynamics*, McGraw Hill Companies, Inc., New York, 2001.

41 Q. B. Fu, Synthesis and properties of 1,1-diamino-2,2-dinitroethylene, PhD thesis, Sichuan Univ., Chengdu, 2007.

42 P. G. Boswell, On the calculation of activation energies using a modified Kissinger method, *J. Therm. Anal.*, 1980, **18**(2), 353–358.

43 Z. M. Fu, J. Y. Huang, X. M. Qian and C. G. Feng, The Research of Thermal Stability of Chemicals by Accelerating Rate Calorimeter, *Fire Saf. Sci.*, 2001, **10**(3), 149–153.

44 W. Liu, Z. X. Liu, J. L. Wang, D. L. Cao and L. Z. Chen, Adiabatic decomposition analyses of 3,4-dinitropyrazole by accelerating rate calorimeter, *Sci. Technol. Eng.*, 2018, **18**(14), 121–125.

45 S. J. Chu, *Thermal Analyses of Explosives*, Science Press, Beijing, 1994.